Second Workshop of DAAD Thematic Network

Universität Stuttgart

Seasonal signals induced by monument thermal effects: Evidence in GPS position time series of short baselines

KH Wang[1,2], WP Jiang[1], H Chen[1], XD An[1], XH Zhou[1], P Yuan[1,2], QS Chen[1]

1 GNSS center, Wuhan University

2 Institute of Geodesy, University of Stuttgart

2018. 07

Content

What is the origin of seasonal signals in GPS position time series ?

- The origins can be divided into two categories:

  - **Artificial/spurious variations**
    - ✓ GPS systematic (orbits, draconitic year)
    - ✓ Reference frame
    - ✓ Mis-modeling errors (HOI, multipath, PCV)
    - ✓ Aliasing of daily/subdaily signal
    - ✓ ……

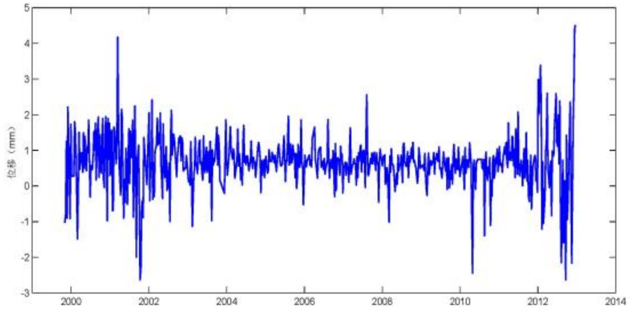

- Partial erased by applying proper processing strategy and models

What is the origin of seasonal signals in GPS position time series ?

- The origins can be divided into two categories:

  - **Real site/monument motions**
    - ✓ Tides (solid, ocean, atmospheric)
    - ✓ Loadings (non-tidal ocean and atm. , CWSL)
    - ✓ Monument thermal effect
    - ✓ Bedrock thermal effect (thermal loading)
    - ✓ ...

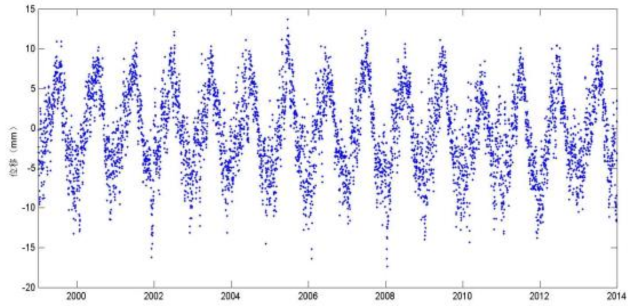

Related to temperature variation

- CANOT BE ELIMINATED! It should be well modeled and quantified.

How to deal with the seasonal signal in GPS position time series ?

- Mathematic model (Bogusz and Klos, 2016):

$$
\begin{aligned}
x(t) = x_0 + v_x \cdot t &+ A^{13.66} \cdot \sin(\omega^{13.66} \cdot t + \phi^{13.66}) \\
&+ A^{14.6} \cdot \sin(\omega^{14.6} \cdot t + \phi^{14.6}) \\
&+ A^{14.19} \cdot \sin(\omega^{14.19} \cdot t + \phi^{14.19}) \\
&+ A^{14.76} \cdot \sin(\omega^{14.76} \cdot t + \phi^{14.76}) \\
&+ \sum_{i=1}^{9} \left[A_i^{CH} \cdot \sin\left(\omega_i^{CH} \cdot t + \phi_i^{CH}\right)\right] \\
&+ \sum_{i=1}^{9} \left[A_i^{T} \cdot \sin\left(\omega_i^{T} \cdot t + \phi_i^{T}\right)\right] \\
&+ \sum_{i=1}^{9} \left[A_i^{D} \cdot \sin\left(\omega_i^{D} \cdot t + \phi_i^{D}\right)\right] + \varepsilon_x(t)
\end{aligned}
$$

Chandler period

Tropical year cycle (365.2days)

GPS draconitic cycle (356.1days)

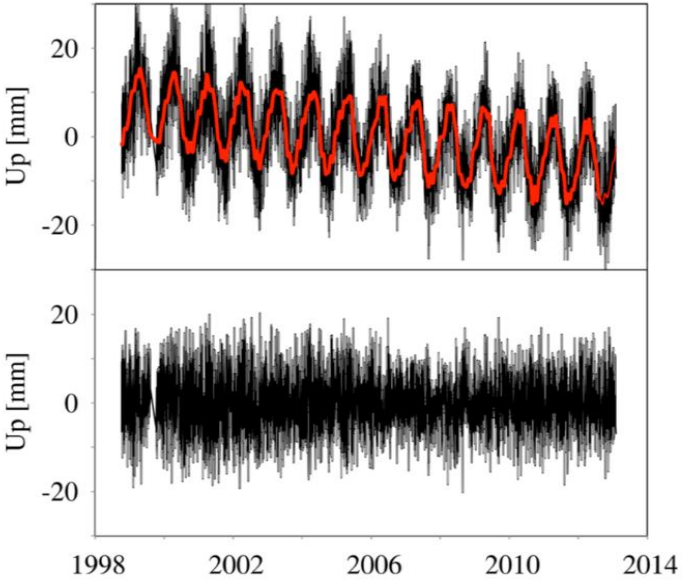

- Good fit in shape, but it is hard to explain the signals by known geophysical process.

How to deal with the seasonal signal in GPS position time series ?

- Geophysical models: corrected and removed from GPS observations

  - ✓ ATML (atmospheric pressure, 5-15 mm)
  - ✓ NTOL (ocean bottom pressure, <5 mm)
  - ✓ CWSL (mass storage, >10 mm)

Limited precision compared to GPS

IGS stations with RMS reduced after corrections (Xu et al., 2017)

Region	Mass-loading	Mass-loading plus thermoelastic of this research
North America	44	51
South America	42	54
Eurasian	39	44
Africa	40	45
Oceania	43	48
Global area	43	50
Sites with positive ratio	71	70

- There are still >30% of the annual variations CANNOT be explained by known contributors in the global scale.
- One of the possible sources is thermal effect of monument (TEM).

What is the problem in the recent analysis of TEM ?

- The thermal signal will be overwhelmed by loading signals, which can bias the quantitative results

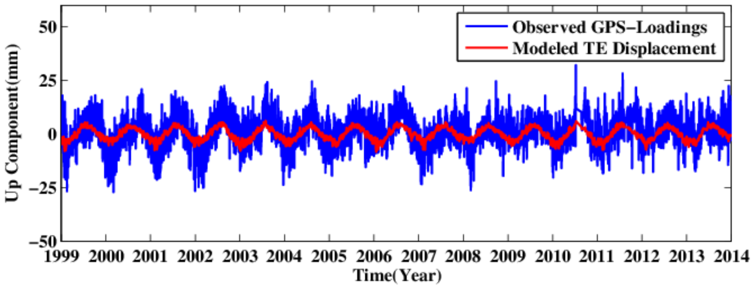

The correction by thermal effect

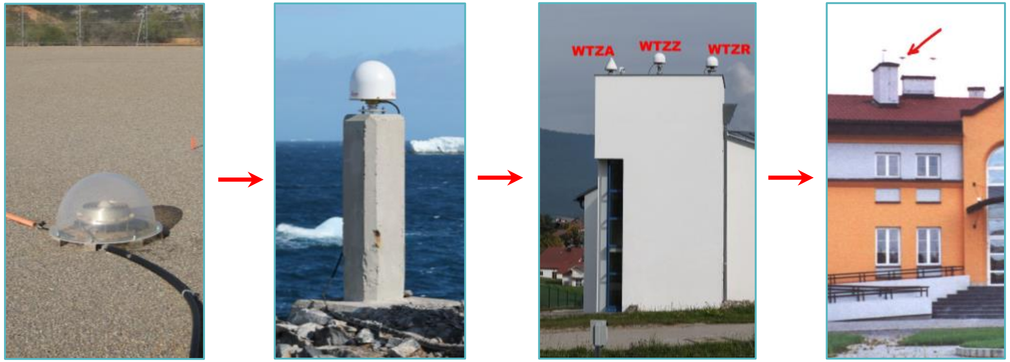

Level 0 Level 1 Level 2 Level 3

- Current models of TEM are still imperfect to explain the rest of the seasonal signal in GPS position time series

What do we do ?

- Analysis based on GPS short-baseline time series:

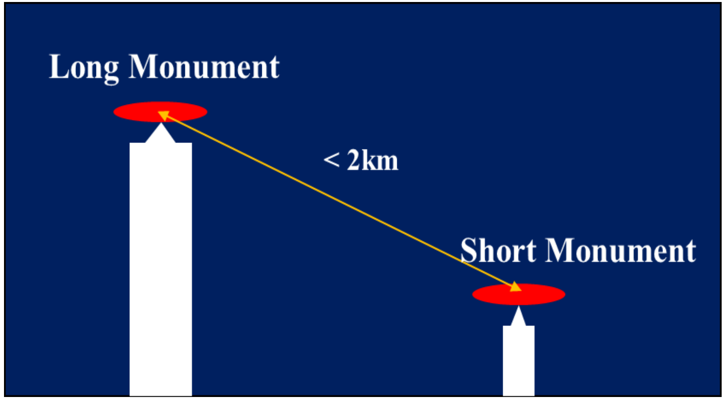

GPS short-baseline adopted

- GPS systematic errors: mostly **differenced**
- Large-scale geophysical effects: **identical**
- Errors related to reference frame: **not exist**
- Time series: **high-precision, stable**

- The remaining: signal by site-specific effects such as TEM, other mis-modeling errors and noise.

Content

☐ Selection of GPS short-baselines

- monument height difference >5 m: Enlarge the thermo-induced signal
- baseline length <1100 m and elevation difference <120 m:
- IGS stations with continuous observations of 2-14 years
- An approximate zero-baseline with identical monument for comparison

Selection of GPS short-baselines

Tab.2 GPS baseline information

Station		Length (m)	Diff. E[b]. (m)	Lon. (deg)	Lat. (deg)	Monument			Common Dataset
						Base	Height[c]	Type[d]	
Experimental group	TCMS[a] TNML	6	0	121.0	24.8	Roof Roof	1.9 2.1	SM SM	2005.001-2014.365
	ZIMJ[a] ZIMM	14	5.1	7.5	46.9	Roof Bedrock	4.0 10.7	CP SM	2003.001-2010.295
	JOZ2[a] JOZE	83	11.1	21.0	52.1	Roof Bedrock	3.5 16.5	CP CP	2002.295-2016.239
	HERT[a] HERS	136	6.9	0.3	50.9	Roof Bedrock	5.5 12.0	CP SM	2003.078-2016.239
	OBE2[a] OBET	268	3.5	11.3	48.1	Roof Roof	4.5 10.0	CP CP	2003.160-2005.129
	MCM4[a] CRAR	1100	117.9	166.7	-77.8	Bedrock Roof	0.1 7.5	CP SM	2002.169-2016.239
Control Group	REYK[a] REYZ	1	0	338.0	64.1	Roof Roof	13.5 13.5	CP CP	2000.001-2007.261

GPS data processing strategies and GPS time series pre-processing

- baseline processing with GAMIT
- 30s sampling interval
- L1_ONLY (LC_AUTCLN for MCCR)
- daily solutions by Kalman-filter
- elevation cutoff of 15°
- final precise satellite orbits from IGS
- zenith tropospheric delay: not estimated except for MCCR (estimated every 2 hour)

- remove outliers: an absolute tolerance of 0.01 m and 0.015m from the median for the horizontal and vertical component or formal errors >0.1 m for any component
- remove accidental errors beyond threshold of 4δ
- moving average over 15 days

Content

☐ Linear trend and residual RMS of each short-baseline

Tab.3 Linear Trend and Residual RMS Estimates of Each Short-baseline

Baseline	Linear Trend (mm/yr)[a]				Residual RMS (mm)			
	N	E	U	L	N	E	U	L
TCTN	-0.14 ± 0.00	-0.04 ± 0.00	0.09 ± 0.00	0.09 ± 0.00	0.2	0.3	0.3	0.3
ZIZI	-0.10 ± 0.02	-0.01 ± 0.02	0.26 ± 0.02	0.06 ± 0.02	1.2	1.2	1.0	1.1
JOJO	0.07 ± 0.00	0.10 ± 0.01	-0.23 ± 0.01	-0.09 ± 0.01	0.6	1.8	1.7	1.2
HEHE	-0.24 ± 0.00	0.23 ± 0.01	0.41 ± 0.01	-0.24 ± 0.01	0.7	0.8	1.0	0.8
OBOB	0.32 ± 0.12	0.01 ± 0.17	-0.36 ± 0.19	-0.27 ± 0.17	0.8	1.1	1.3	1.2
MCCR	-0.74 ± 0.01	0.39 ± 0.01	-0.04 ± 0.02	-0.73 ± 0.01	0.8	0.9	2.4	0.8
RERE	0.26 ± 0.01	-0.07 ± 0.01	0.43 ± 0.02	0.21 ± 0.01	0.6	0.7	1.2	0.7

- There are apparent trends in the time series, even for the short-baselines!
- The distance of MCCR located in the Antarctica is closing by 0.7 mm/yr

◻ De-trended time series of GPS short-baselines (1)

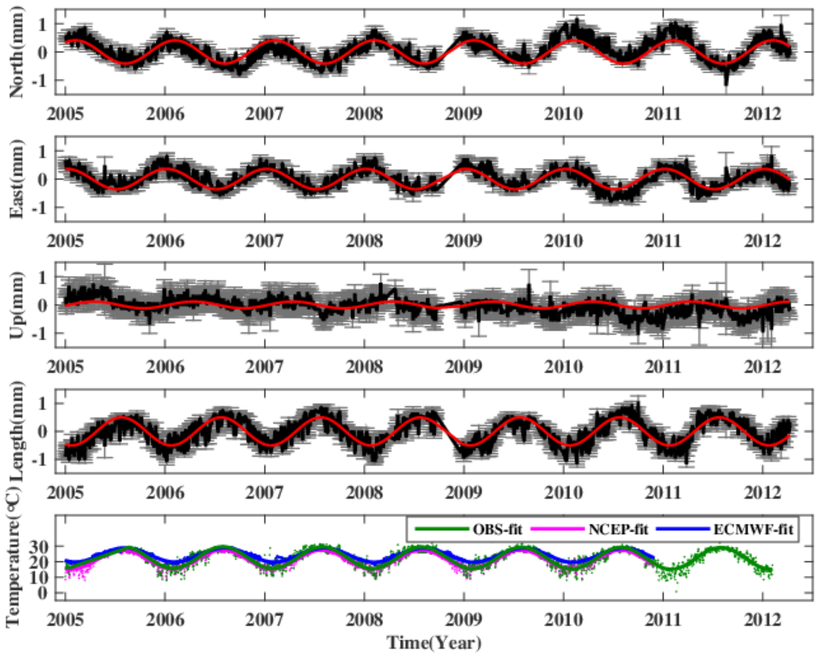

GPS short-baseline TCTN (length: 6 m)

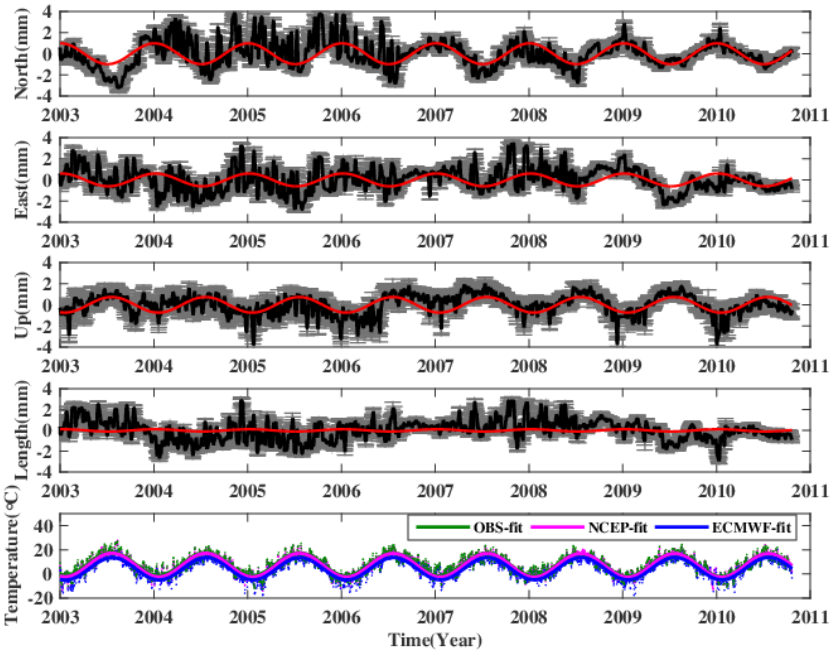

GPS short-baseline ZIZI (length: 14 m)

◻ De-trended time series of GPS short-baselines (2)

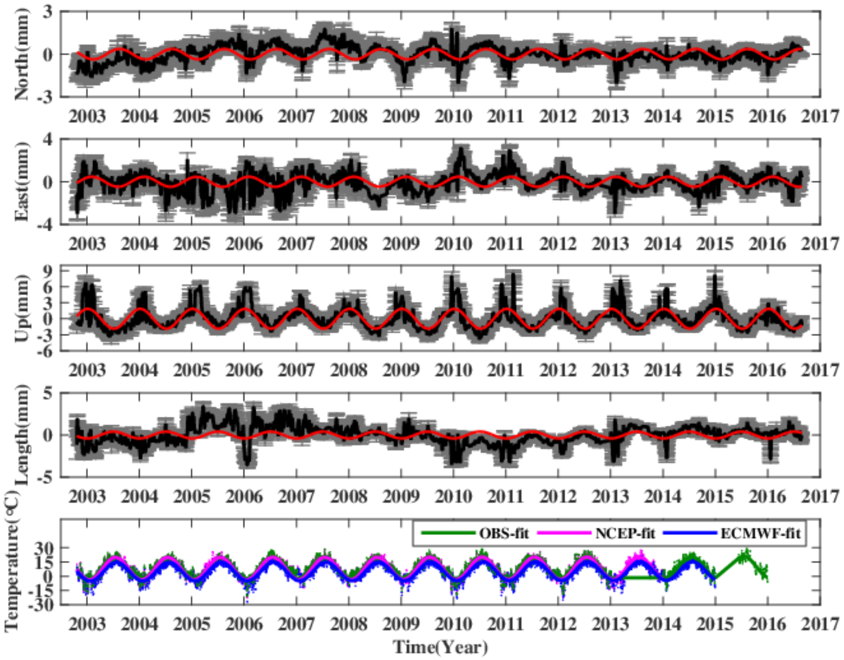

GPS short-baseline JOJO (length: 83 m)

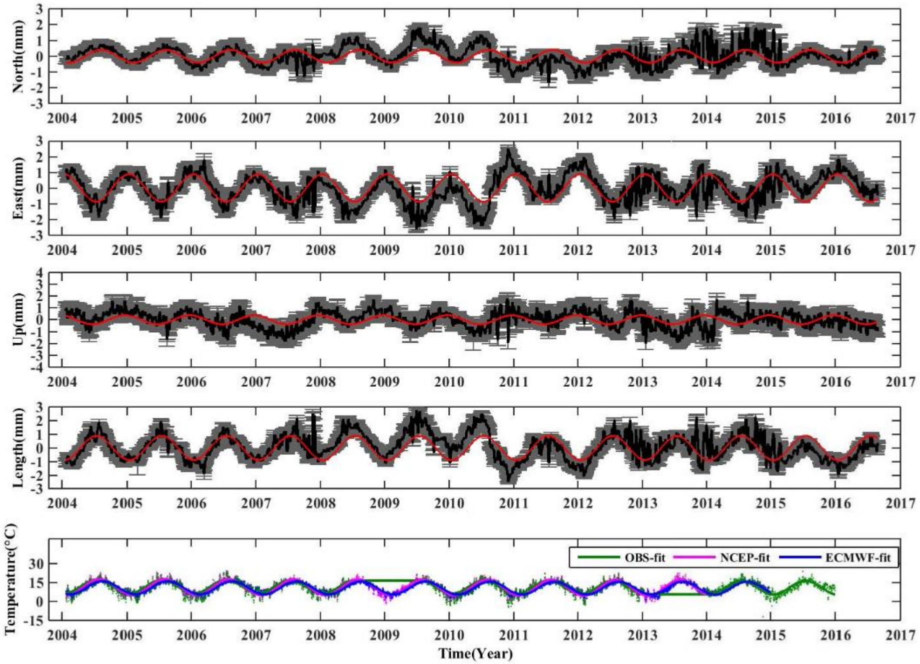

GPS short-baseline HEHE (length: 136 m)

◻ De-trended time series of GPS short-baselines (3)

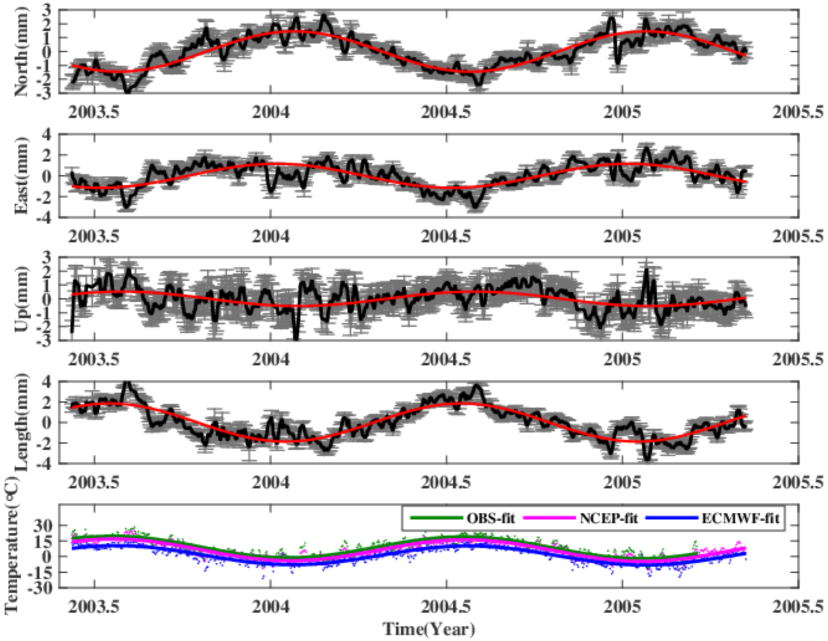

GPS short-baseline OBOB (length: 268 m)

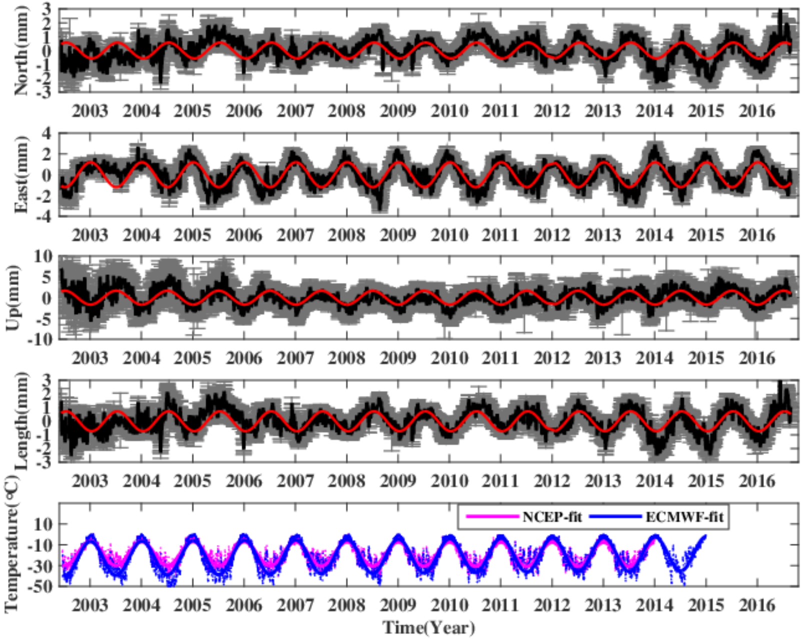

GPS short-baseline MCCR (length: 1100 m)

◻ De-trended time series of GPS short-baselines (4)

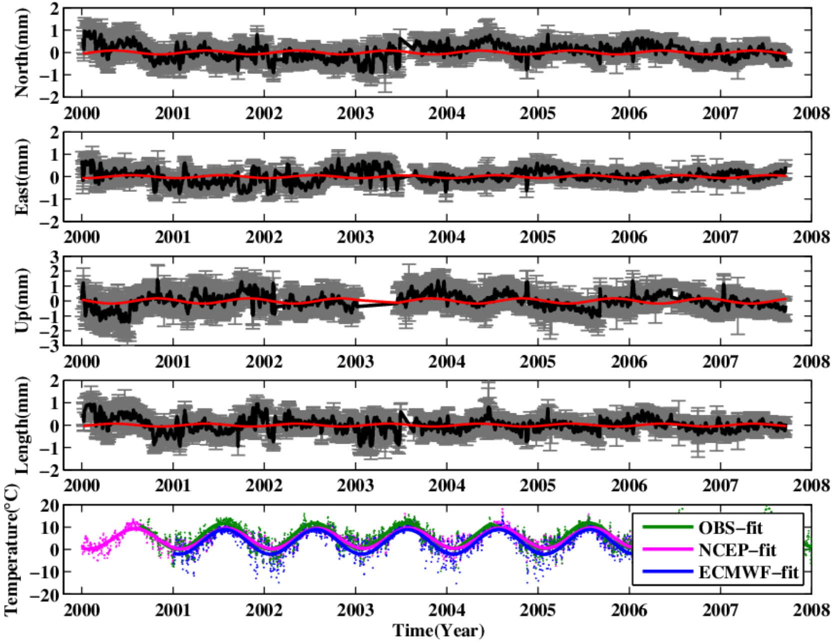

GPS short-baseline RERE (length: <1m)

Almost all of the components of the GPS short-baselines with apparent monument height difference exhibit ***strong annual oscillation***, the time series reach to extremum in January during the winter or in July during the summer

◻ Spectral analysis

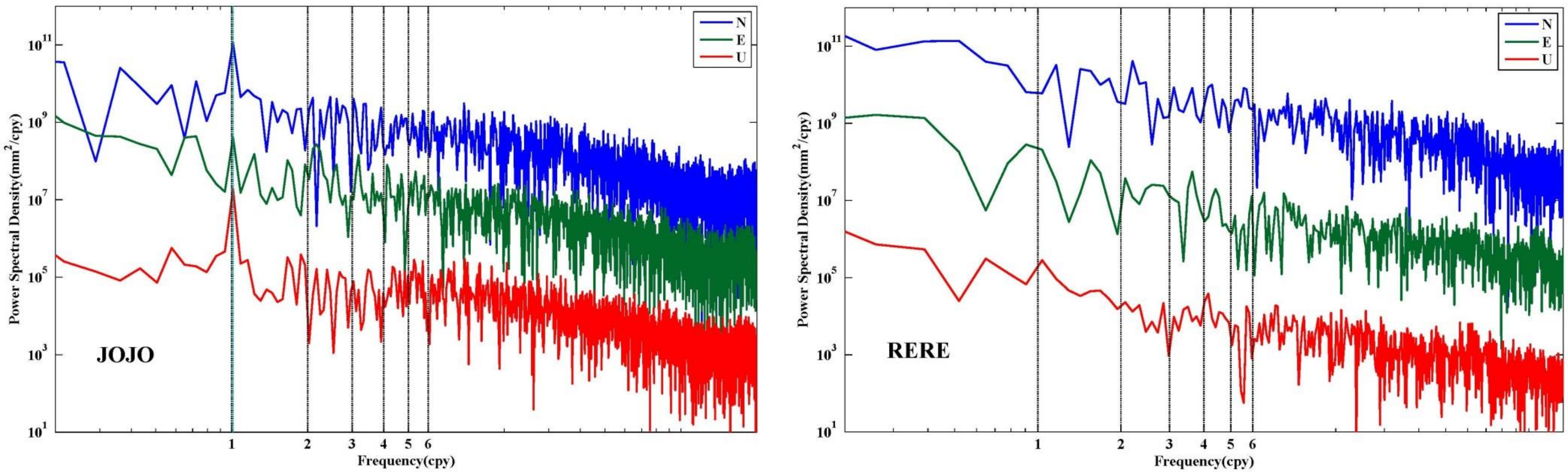

Power spectral density (PSD) values for each component of the baselines. PSD values for the N and E component are isolated by adopting appropriate scale factors.

- all with annual cycle (except RERE), semiannual occurs on partial components

☐ Seasonal signals

$$y = a \cdot t + b + A_1 \cos(2\pi \cdot t + \varphi_1) + A_2 \cos(4\pi \cdot t + \varphi_2) + \epsilon$$

- Max A.A. : **1.86 ± 0.17 mm**
  Median: 0.64 ± 0.13mm
- Max SA.A. : **0.71 ± 0.14 mm**
  Median: 0.12 ± 0.14mm
- **78%** (14/18) are in phase (±15°) with local temperature
- negligible amplitude for baseline RERE

Tab.5 Amplitudes and phases estimates

Baseline		Annual Amplitude (mm)	Annual Phase (degree)	Semiannual Amplitude (mm)	Semiannual Phase (degree)	Annual Temperature Variation (℃)	Annual Temperature Phase (degree)
TCTN	N	0.42 ± 0.03	*146 ± 4**	0.05 ± 0.02	-19 ± 23	7.0 ± 0.1	152 ± 1
	E	0.35 ± 0.03	171 ± 5*	0.04 ± 0.02	-25 ± 27		
	U	0.13 ± 0.02	74 ± 9	0.00 ± 0.00	-		
	L	0.45 ± 0.04	*155 ± 5**	-	-		
ZIZI	N	**1.04 ± 0.13**	*174 ± 7**	0.24 ± 0.13	-50 ± 24	9.5 ± 0.2	162 ± 1
	E	0.63 ± 0.10	*174 ± 8**	0.34 ± 0.08	-30 ± 13		
	U	1.04 ± 0.20	*166 ± 11*	0.20 ± 0.14	26 ± 40		
	L	0.11 ± 0.14	*172 ± 8**	-	-		
JOJO	N	0.29 ± 0.10	134 ± 19	0.14 ± 0.44	-39 ± 35	11.3 ± 0.2	165 ± 1
	E	0.39 ± 0.16	*160 ± 24**	0.12 ± 0.12	-32 ± 57		
	U	**1.86 ± 0.17**	*170 ± 5**	0.97 ± 0.25	-46 ± 15		
	L	0.41 ± 0.15	*178 ± 17*	-	-		
HEHE	N	0.40 ± 0.06	142 ± 8	0.04 ± 0.18	50 ± 45	5.4 ± 1.9	167 ± 21
	E	**0.96 ± 0.07**	*173 ± 4**	0.11 ± 0.06	-42 ± 30		
	U	0.41 ± 0.06	194 ± 6*	0.14 ± 0.04	-22 ± 17		
	L	**0.92 ± 0.05**	*168 ± 2*	-	-		
OBOB	N	**1.17 ± 0.13**	*155 ± 6**	0.43 ± 0.13	-6 ± 22	10.2 ± 0.5	162 ± 3
	E	**1.18 ± 0.12**	*175 ± 6**	0.48 ± 0.12	-24 ± 14		
	U	0.65 ± 0.16	*155 ± 14*	0.28 ± 0.15	-22 ± 14		
	L	**1.86 ± 0.13**	*165 ± 8*	-	-		
MCCR	N	0.59 ± 0.03	*346 ± 3**	0.05 ± 0.06	-7 ± 39	16.4 ± 0.3	357 ± 1 (South)
	E	**1.32 ± 0.07**	*355 ± 3*	0.39 ± 0.07	47 ± 10		
	U	**1.62 ± 0.14**	*358 ± 5**	0.71 ± 0.14	-10 ± 12		
	L	0.73 ± 0.08	*349 ± 3**	-	-		
RERE	N	0.14 ± 0.10	10 ± 39	0.12 ± 0.21	-6 ± 43	5.8 ± 0.2	161 ± 2
	E	0.10 ± 0.18	44 ± 11	0.12 ± 0.16	-32 ± 81		
	U	0.28 ± 0.19	83 ± 37	0.15 ± 0.24	-42 ± 27		
	L	0.08 ± 0.09	149 ± 29	-	-		

◻ Time-correlated noise

- FN: flicker + white noise
- RW: random-walk + white noise
- PL: power-law + white noise
- FNRW: flicker + random-walk + white noise
- BPPL: band-pass-filtered+ power-law + white noise
- BPRW: band-pass-filtered+ random-walk + white noise
- FOGMRW: first-order Gauss-Marcov + random-walk + white noise

◻ The ONM (Optimal Noise Model) for the stochastic process

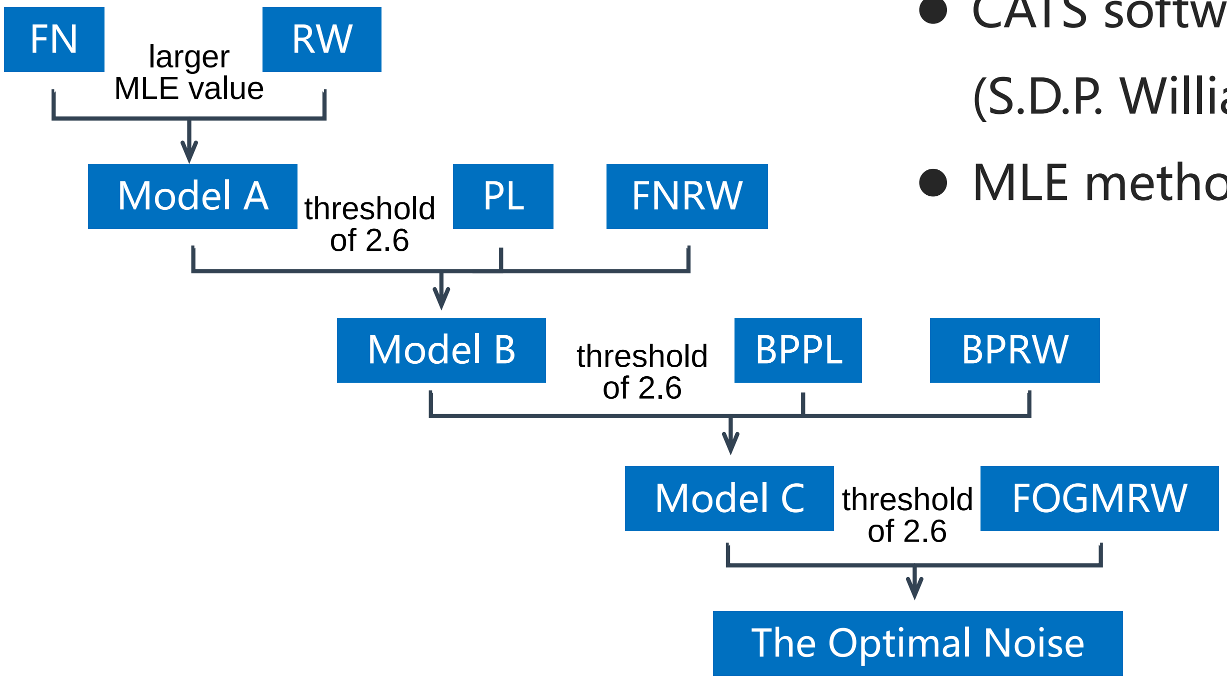

The procedure of choosing the ONM

- CATS software package v3.1.2 (S.D.P. Williams)
- MLE method from *Langbein* [2004]

☐ Noise characteristics

- Instead of FN or RW, BP noise is valid for ~40% of the baseline components, and another 20% can be best modeled by a combination of FOGM process plus WN

Tab.4 Statistics of the ONM and relevant parameters estimated

		TCTN	ZIZI	JOJO	HEHE	OBOB	MCCR	RERE
N	ONM[a]	***PL***	***BPPL***	***FL***	***FOGMRW***	***BPRW***	***FL***	***RW***
	A.CN[b]	PL: 0.64 ± 0.01	BP: 0.12 ± 0.01 PL: 2.62 ± 0.11	FL: 1.66 ± 0.31	FOGM: 9.90 ± 0.27 RW: 0.86 ± 0.09	BP: 4.79 ± 0.72 RW: 0.00 ± 0.00	FL: 1.74 ± 0.13	RW: 0.54 ± 0.18
	A.WN	0.00 ± 0.00	0.00 ± 0.00	3.69 ± 0.04	0.34 ± 0.01	2.12 ± 0.06	1.47 ± 0.02	3.11 ± 0.04
	NP[c]	Index: -1.12	Index: -1.01	Index: -1	Beta: 206.04	F: 4.32 W: 0.70 N: -7.26	Index: -1	Index: -2
E	ONM[a]	***FLRW***	***FOGMRW***	***FL***	***FL***	***BPRW***	***PL***	***RW***
	A.CN[b]	FL: 0.59 ± 0.01 RW: 0.21 ± 0.06	FOGM: 20.92 ± 0.68 RW: 0.69 ± 0.16	FL: 4.40 ± 0.29	FL: 1.90 ± 0.13	BP: 0.10 ± 0.01 RW: 0.00 ± 0.00	PL: 4.05 ± 0.04	RW: 1.00 ± 0.29
	A.WN	0.00 ± 0.00	0.60 ± 0.04	2.52 ± 0.04	1.37 ± 0.02	1.15 ± 0.04	0	5.79 ± 0.08
	NP[c]	-	Beta: 166.9	Index: -1	Index: -1	F: 2.46 W: 0.05 N: 3.13	Index: -0.11	Index: -2
U	ONM[a]	***FLRW***	***BPPL***	***BPPL***	***FOGMRW***	***BPRW***	***PL***	***BPRW***
	A.CN[b]	FL: 0.43 ± 0.02 RW: 0.15 ± 0.04	BP: 0.11 ± 0.01 PL: 4.01 ± 0.19	BP: 0.61 ± 0.09 PL: 7.92 ± 1.65	FOGM: 10.99 ± 0.54 RW: 0.94 ± 0.10	BP: 0.37 ± 0.05 RW: 0.00 ± 0.00	PL: 0.01 ± 0.00	BP: 1.89 ± 0.21 RW: 5.77 ± 0.65
	A.WN	0.10 ± 0.00	0.00 ± 0.00	1.23 ± 4.31	0.81 ± 0.02	1.86 ± 0.06	7.05 ± 0.07	3.98 ± 0.06
	NP[c]	-	Index: -1.01	Index: -0.27	Beta: 224.63	F: 3.47 W: 0.25 N: -4.90	Index: -6.05	F: 0.45 W: 0.34 N: 2.96

Comparison with previous researches (King and Williams, 2009; Wilkinson et al., 2013)

- Regardless of the slight difference in GPS process strategy, amplitudes seem to be consistent with each other
- Minor uncertainty compared to results of King and Williams[2009] in general (due to longer time span and more proper noise models)

Tab.5 Amplitudes and phases estimates

Baseline	Components		*King and Williams*, 2009	*Wilkinson* et al., 2013	This paper
HEHE	annual	N	0.54 ± 0.10	0.50 ± 0.01	0.40 ± 0.06
		E	1.04 ± 0.16	1.05 ± 0.01	0.96 ± 0.07
		U	0.30 ± 0.22	0.42 ± 0.00	0.41 ± 0.06
	semiannual	N	0.03 ± 0.08	-	0.04 ± 0.18
		E	0.20 ± 0.12	-	0.11 ± 0.06
		U	0.03 ± 0.16	-	0.14 ± 0.04
ZIZI	annual	N	1.08 ± 1.46	-	1.04 ± 0.13
		E	0.59 ± 1.34	-	0.63 ± 0.10
		U	0.68 ± 0.38	-	1.04 ± 0.20
	semiannual	N	0.29 ± 0.88	-	0.24 ± 0.13
		E	0.30 ± 0.80	-	0.34 ± 0.08
		U	0.21 ± 0.28	-	0.20 ± 0.14
JOJO	annual	N	0.17 ± 0.14	-	0.29 ± 0.10
		E	0.36 ± 0.18	-	0.39 ± 0.16
		U	2.25 ± 0.92	-	1.86 ± 0.17
	semiannual	N	0.16 ± 0.10	-	0.14 ± 0.44
		E	0.17 ± 0.12	-	0.12 ± 0.12
		U	0.99 ± 0.56	-	0.97 ± 0.25

Content

a) Thermal expansion of the monument (TEM) and bedrock (TEB)

□ For the vertical direction

- TEM (an improved model)

Thermal-induced deformation of medal or concrete material

$$\Delta L(t) = \alpha \cdot h \cdot [T(t) - T']$$

■ $h = h_1 + h_2$, considering the structure beneath antenna and underground

- TEB (adopt from Yan et al., 2009)

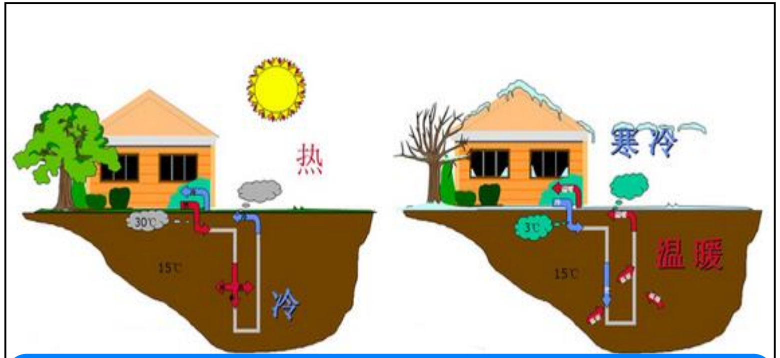

Thermal elastic response of the shallow crust, which can be regarded as thermal loading

$$T(t) = T_0 + \sum_{n=1}^{\infty} (a_n \cos wt + b_n \sin wt)$$

$$\text{TEB:}\quad \Delta h(t) = \frac{1+\mu}{1-\mu} \alpha \sum_{i=1}^{N} a_i \sqrt{\frac{\kappa}{b_i}} \cos\left(b_i t + c_i - \frac{\pi}{4}\right)$$

◻ For the vertical direction

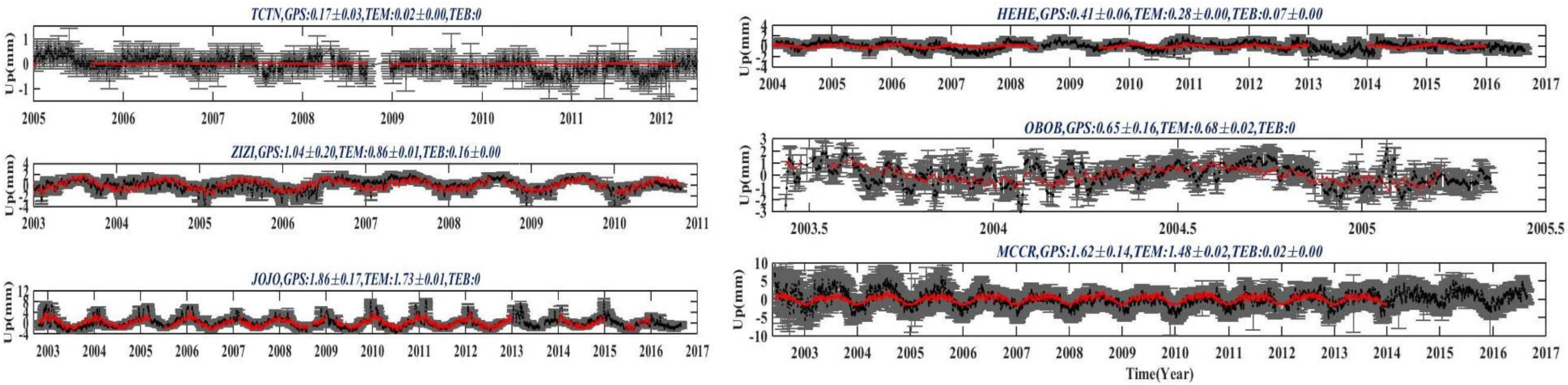

The modeled thermo-induced displacements (TEM+TEB) and the observed GPS time series

- Good fit between the observed GPS and the modeled TEM+TEB time series, especially for baselines with apparent seasonal amplitudes

For the vertical direction

Tab.6 Amplitude and phase estimates of the MTE displacements and observed GPS time series

Baselines		TCTN	ZIZI	JOJO	HEHE	OBOB	MCCR	RERE
A.A	U	0.13 ± 0.02	1.04 ± 0.20	1.86 ± 0.17	0.41 ± 0.06	0.65 ± 0.16	1.62 ± 0.14	0.28 ± 0.19
	TEM	0.02 ± 0.00	0.86 ± 0.01	1.73 ± 0.01	0.28 ± 0.00	0.68 ± 0.02	1.48 ± 0.02	0
	TEB	0	0.16 ± 0.00	0	0.07 ± 0.00	0	0.02 ± 0.00	0
	ratio	15.4%	84.1%	93.0%	70.4%	104.6%	91.4%	0
A.P	U	74 ± 9	-14 ± 11	-10 ± 5	14 ± 9	-25 ± 14	-20 ± 5	83 ± 37
	TEM	-20 ± 1	-18 ± 1	-13 ± 2	-25 ± 1	-19 ± 1	-23 ± 1	0
	TEB	0	-63 ± 0	0	-70 ± 0	0	0	0
S.A.A	U	0.00 ± 0.00	0.20 ± 0.14	0.97 ± 0.25	0.14 ± 0.04	0.28 ± 0.15	0.71 ± 0.14	0.15 ± 0.24
	TEM	0	0.02 ± 0.01	0.07 ± 0.08	0.01 ± 0.01	0.06 ± 0.03	0.18 ± 0.02	0
	TEB	0	0	0	0	0	0	0
	ratio	-	10.0%	7.2%	7.1%	21.4%	25.4%	0
S.A.P	U	-	26 ± 40	-46 ± 15	-22 ± 16	-22 ± 14	-10 ± 12	-42 ± 27
	TEM	-	59 ± 34	74 ± 24	-76 ± 12	-52 ± 15	-14 ± 2	0
	TEB	-	0	0	0	0	0	0

- Median annual amplitude ratio ((TEM+TEB)/GPS)) is ~88% for the test group
- Median semi-annual amplitude ratio is 9%
- Median contribution is **88% vs. 46%** with and without considering the extra parts of the monument, respectively

◻ For the horizontal directions

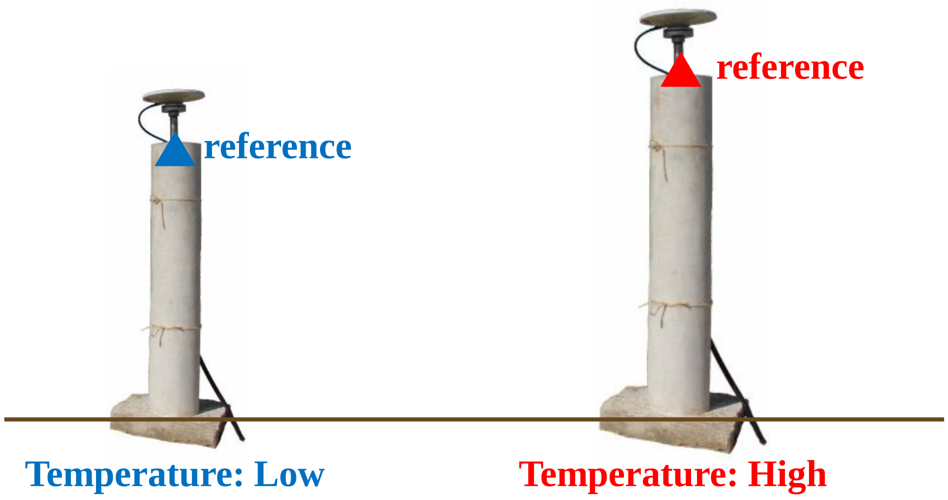

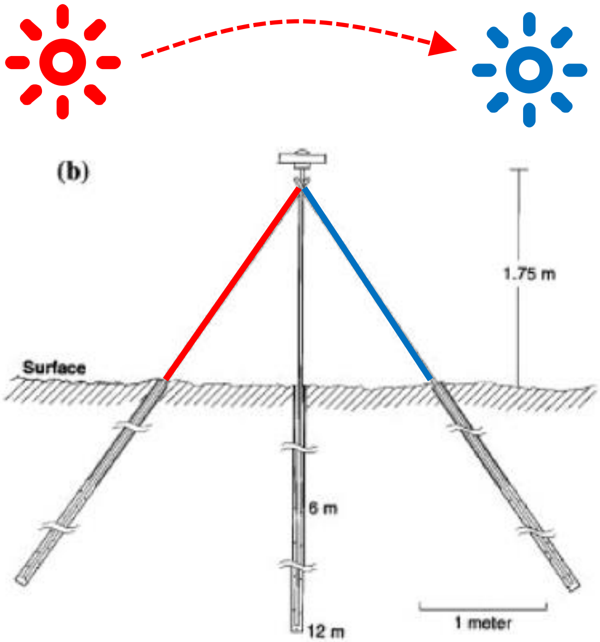

The diagrammatic sketch of daily monument deformation

- As the homogeneous structure of the monument, there seems slight seasonal oscillation on the horizontal direction induced by TEM

□ For the horizontal directions

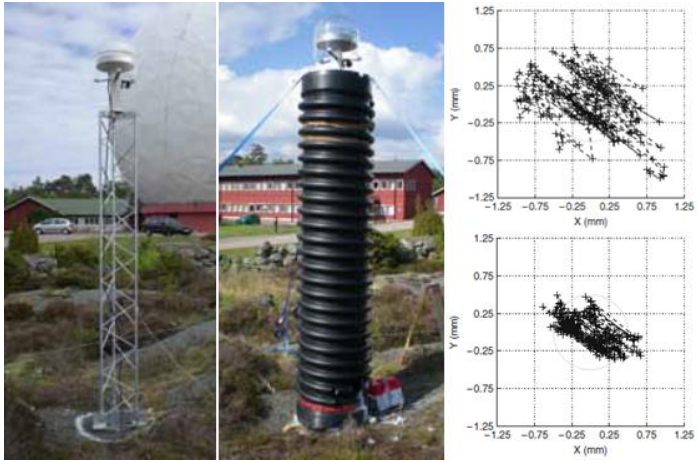

The steel trust monument with and without insulated pipe and the corresponding displacements (from Lehner, 2011).

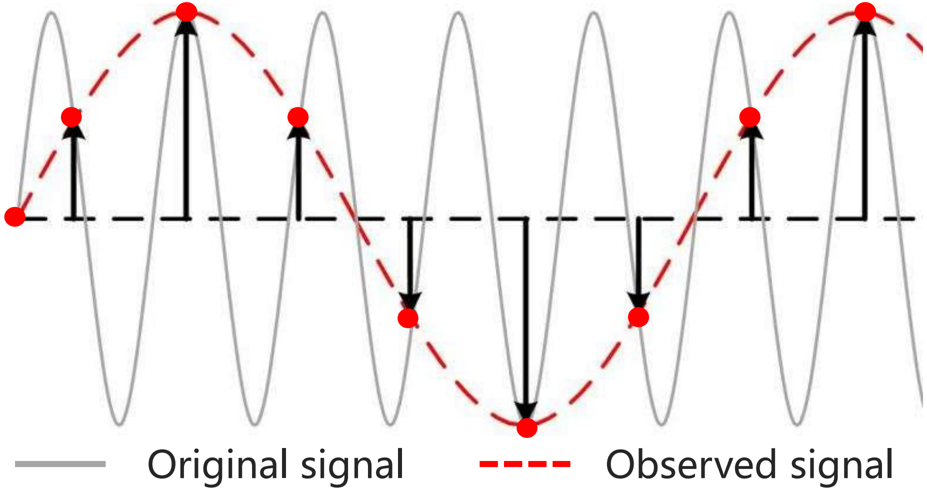

The aliasing of sub-daily signal to long-term periodical signal, such as annual cycle

- Daily/subdaily MTE displacements also exist in total station observations (Haas et al., 2013), and the oscillation can be **3 mm during summer**

b) The spurious seasonal signal induced by tropospheric delay error

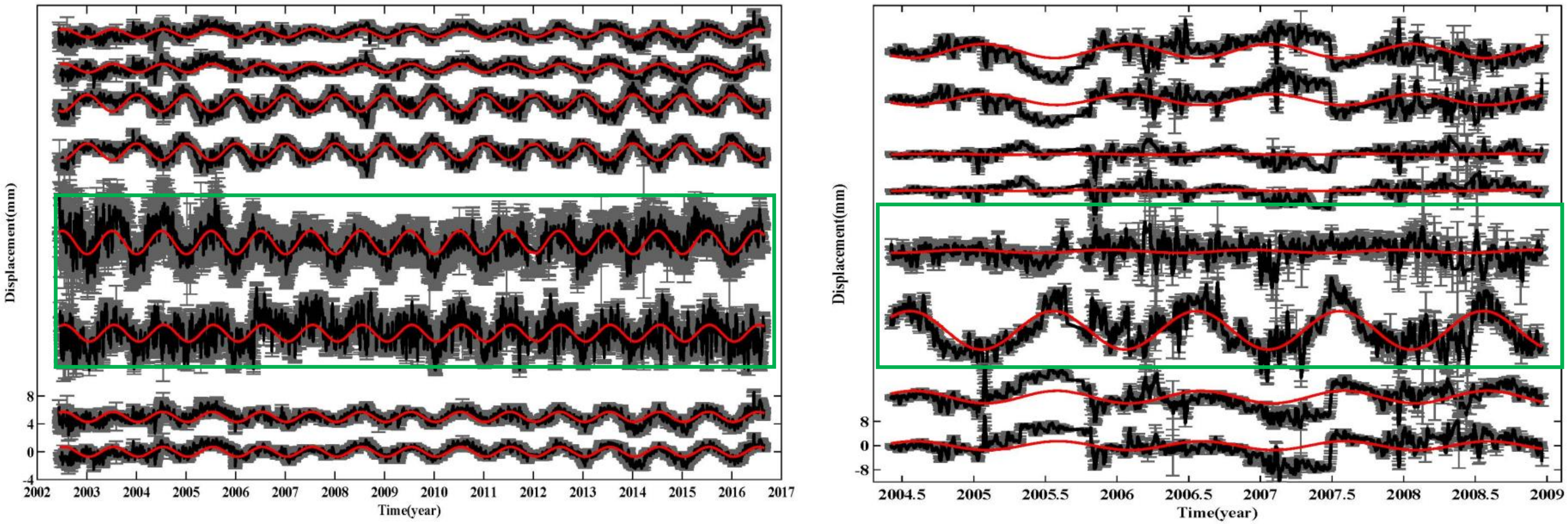

Fig.19 GPS residuals of MCCR(left) and PEPE(right) with and without tropospheric delay estimated

- The spurious annual amplitude induced by tropospheric delay modeling error is **~4.8 mm** and **~1.8 mm** for MCCR and PEPE, respectively

c) Variations induced by site environment

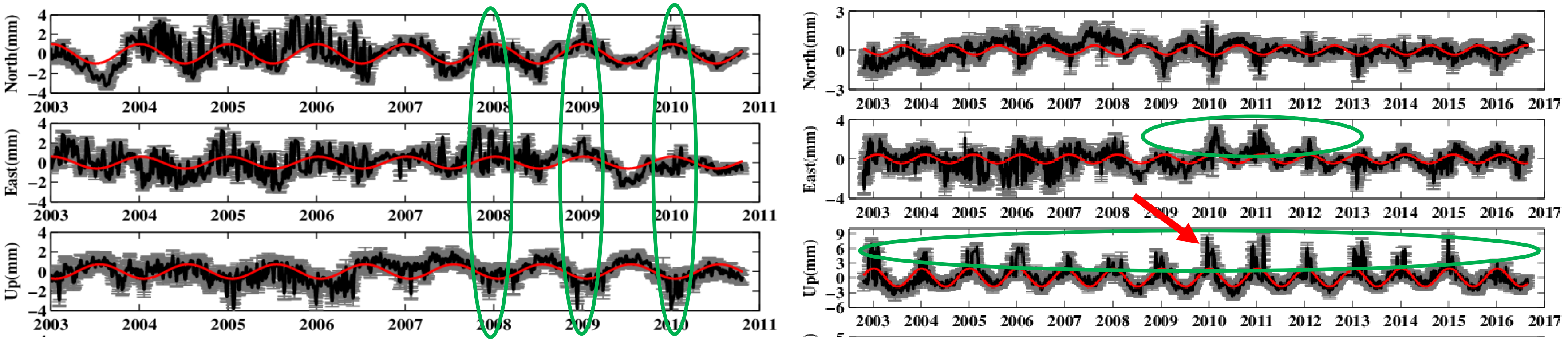

GPS residuals of ZIZI(left) and JOJO(right)

- JOJO: oscillation is ~8 mm from December to the end of February next year during 2003 to 2015, similar phenomenon occurs in Track solution of King and Williams [2009] and PPP solution of Wu et al., [2013]
- May be a sort of systematic error and related to site environment such as signal delay error induced by snow over the GPS antenna

Content

Conclusions

- Apparent seasonal signals with annual amplitude of ~1mm (maximum amplitude of 1.86 ± 0.17mm) are detected on almost all components, obvious annual signals (amplitude >1 mm) in the horizontal direction are also observed in 4/5 short-baselines.
- Thermal effect of monument can explain 46% of the vertical annual amplitude of GPS baseline solutions, and the ratio increases to 84% when taking the without additional parts of the monument into account.
- Mismodeling of the tropospheric delay may also introduce spurious annual amplitudes of ~5mm and ~2 mm, respectively, for two short-baselines with elevation differences greater than 100 m.
- The conclusions can help to better understand the mechanism of seasonal signal in GPS position time series.

Future Work

- The origins of the obvious annual and semiannual signals on the horizontal components still need further investigation.
- Aliasing of the daily or subdaily displacements induced by thermal effect of the monument should be investigated further based on sampling interval larger than a single day.
- Other potential contributors to seasonal or diurnal signals.

Thanks for your attention!

Any questions?